Journal of Solid Mechanics Vol. 7, No. 2 (2015) pp. 158-172

Free Vibration Analyses of Functionally Graded CNT Reinforced Nanocomposite Sandwich Plates Resting on Elastic Foundation

R. Moradi-Dastjerdi [1, *], Gh. Payganeh [2], H. Malek-Mohammadi [2]

[1] *Young Researchers and Elite Club, Khomeinishahr Branch, Islamic Azad University, Khomeinishahr, Iran*
[2] *School of Mechanical Engineering, Shahid Rajaee Teacher Training University, Tehran, Iran*

Received 22 February 2015; accepted 12 April 2015

ABSTRACT

In this paper, a refined plate theory is applied to investigate the free vibration analysis of functionally graded nanocomposite sandwich plates reinforced by randomly oriented straight carbon nanotube (CNT). The refined shear deformation plate theory (RSDT) uses only four independent unknowns and accounts for a quadratic variation of the transverse shear strains across the thickness, and satisfies the zero traction boundary conditions on the top and bottom surfaces of the plate without using shear correction factors. The motion equations are derived using Hamilton's energy principle and Navier's method and is applied to solve this equation. The sandwich plates are considered simply supported and resting on a Winkler/Pasternak elastic foundation. The material properties of the functionally graded carbon nanotube reinforced composites (FG-CNTRCs) are graded along the thickness and estimated though the Mori–Tanaka method. Effects of CNT volume fraction, geometric dimensions of sandwich plate, and elastic foundation parameters are investigated on the natural frequency of the FG-CNTRC sandwich plates.

Keywords : Sandwich plates; Mori–Tanaka approach; Refined plate theory; Carbon nanotubes; Navier's solution.

1 INTRODUCTION

RECENTLY, the use of carbon nanotubes in polymer/carbon nanotube composites has attracted wide attention [1]. A high aspect ratio, low weight of CNTs and their extraordinary mechanical properties (strength and flexibility) provide the ultimate reinforcement for the next generation of extremely lightweight but highly elastic and very strong advanced composite materials. On the other hand, by using of the polymer/CNT composites in advanced multilayered composite materials (sandwich structures) we can achieve structures with low weight, high strength and high stiffness in many structures of civil, mechanical and space engineering. Some research papers on material properties of nanocomposite reinforced by CNT are available [2-6]. Also, some investigations show that the mechanical, electrical and thermal properties of these nanocomposites can considerably improve by the addition of small amount of CNT in the matrix [6-9].Molecular dynamic (MD) is one of the techniques that can be used to study on CNTs. Han and Elliott [5] successfully used MD method to determine the elastic modulus of composite structures under CNTs reinforcement and they investigated the effect of CNT volume fraction on mechanical

* Corresponding author. Tel.: +98 913 205 8928.
E-mail address: rasoul.moradi@iaukhsh.ac.ir (R.Moradi-Dastjerdi).

properties of nanocomposites. Wuite and Adali [10] studied about the deflection and stress of nanocomposite reinforced beams by a multi-scale analysis and observed that small amount of nanotube reinforcement significantly improves beam stiffness.

Functionally graded materials (FGMs) are inhomogeneous composites characterized by smooth and continuous variations in both compositional profile and material properties. Such excellent performances allow them to be fabricated as different structures in accordance to various service requirements. To obtain the required optimum performance, the gradient variation of material properties can be achieved by gradually changing the volume fraction of the constituent materials. Reddy [11] presented static and dynamic analysis of the FGM plates based on third order shear deformation theory and by using the theoretical formulation and finite element models. Cheng and Batra [12] used first and third order shear deformation theories to relate deflections of a simply supported functionally graded polygonal plate. Also, Cheng and Batra [13] have studied on the buckling and steady state vibrations of a simply supported functionally graded polygonal plate based on Reddy's plate theory.

The CNTs can be distributed as some grading profiles through a certain direction to improve the mechanical properties and to reinforce the composite structures too. The composites, which are reinforced by CNTs with grading distribution, are called functionally graded carbon nanotube-reinforced composites. Shen [14] suggested that the interfacial bonding strength can be improved through the use of a graded distribution of CNTs in the matrix and investigated postbuckling of functionally graded nanocomposite cylindrical shells reinforced by CNTs subjected to axial compression in thermal environment and showed that the linear functionally graded reinforcements can increase the buckling load. He estimated mechanical properties by a micro-mechanical model in volume fraction form with CNT efficiency parameters. Ke et al. [15] investigated the nonlinear free vibration of FG-CNTRC beams based on von Karman geometric nonlinearity and Timoshenko beam theory. The material properties were assumed to be graded along the thickness and estimated though the rule of mixture. They introduced the CNT efficiency parameter to account for load transfer between the nanotube and polymeric phases. However, the rule of mixture is not applicable when straight CNTs are oriented randomly in the matrix. In these cases the Mori–Tanaka approach [16] is applicable to predict material properties of composites reinforced. Yas and Heshmati [17] used the Mori–Tanaka approach to study on the vibrational properties of FG-nanocomposite beams reinforced by randomly oriented straight CNTs under the action of moving load. Sobhani Aragh et al. [18] presented vibrational behavior of continuously graded CNT–reinforced cylindrical panels based on the Eshelby–Mori–Tanaka approach. They used the 2D Generalized Differential Quadrature Method (GDQM) to discretize the governing equations and to implement the boundary conditions. Also, Pourasghar et al. [19] and Moradi-Dastjerdi et al. [20] investigated free vibrations analysis FG nanocomposite cylinders reinforced by randomly oriented straight and local aggregation CNTs based on three-dimensional theory of elasticity and a mesh-free method, respectively. They estimated material properties of FG- CNTRCs through the Eshelby–Mori–Tanaka approach too.

The simplest model for the elastic foundation is the Winkler model, which regards the foundation as a series of separated springs without coupling effects between each other, resulting in the disadvantage of discontinuous deflection on the interacted surface of the plate. This was later improved by Pasternak [21] who took account of the interactions between the separated springs in the Winkler model by introducing a new dependent parameter. In a new and near work, Pourasghar and Kamarian [22] used the Winkler/Pasternak elastic foundation in their study. They presented free vibrational analyses of FG nanocomposite cylindrical panels reinforced by multiwalled CNTs resting on the Winkler/Pasternak elastic foundation based on the three-dimensional theory of elasticity.

Since the first shear deformation plate theory (FSDT) violates the equilibrium conditions on the top and bottom surfaces of the plate, a shear correction factor is required to compensate for the error due to a constant shear strain assumption through the thickness. The shear correction factor not only depends on the material and geometric properties but also it depends on the loading and boundary conditions. Although the FSDT provides a sufficiently accurate description of response for thin to moderately thick plate, it is not convenient for use due to the difficulty in determination of the correct value of the shear correction factor. To avoid the use of shear correction factor, many RSDTs have been developed such as the sinusoidal shear deformation plate theory (SSDT) [23-24], RSDT [25-26] and hyperbolic shear deformation plate theory (HSDT) [27-29]. RSDT is based on assumption that the in-plane and transverse displacements consist of bending and shear components in which the bending components do not contribute toward shear forces and, likewise, the shear components do not contribute toward bending moments. The motion equation can be derived by using of Hamilton's energy principle and Navier's method solves this equation.

In this work, a RSDT is developed to investigate the free vibration analysis of simply supported FG-CNTRC sandwich plates resting on the Winkler/Pasternak elastic foundation. The material properties of the nanocomposites plates are graded along the thickness and estimated through the Mori–Tanaka method because of its simplicity and accuracy even at a high volume fraction of inclusions. The effects of CNT volume fraction, geometric dimensions of

sandwich plate, and elastic foundation parameters are investigated on the natural frequency of these FG-CNTRC sandwich plates.

2 MATERIAL PROPERTIES IN FG-CNT REINFORCED COMPOSITE

Consider a CNTRC made from a mixture of single-walled CNTs (with randomly orientation) and matrix which is assumed to be isotropic. The single-walled CNT reinforcement is either uniformly distributed (UD) or FG in the thickness of plates. In this section, the effective mechanical properties of these composites are obtained based on the Mori–Tanaka approach. The resulting effective properties for the randomly oriented CNT composite are isotropic, despite the CNTs having transversely isotropic effective properties. The orientation of a straight CNT is characterized by two Euler angles α and β, as shown in Fig. 1. When CNTs are completely randomly oriented in the matrix, the composite is then isotropic, and its bulk modulus K and shear modulus G are derived as [30]:

$$K = K_m + \frac{f_r(\delta_r - 3K_m\alpha_r)}{3(f_m + f_r\alpha_r)}, G = G_m + \frac{f_r(\eta_r - 2G_m\beta_r)}{2(f_m + f_r\beta_r)} \tag{1}$$

where subscripts m and r are referred to matrix and CNT respectively, f is volume fraction and also,

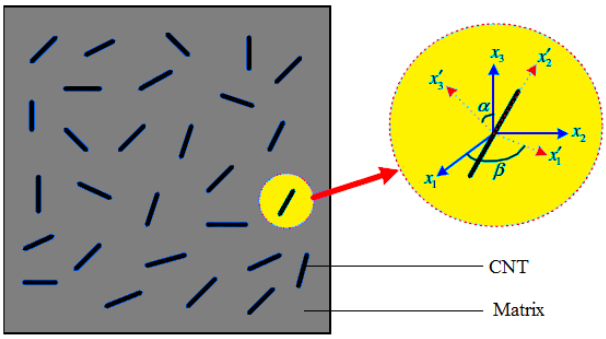

Fig.1
Representative volume element with randomly oriented, straight CNTs [17].

$$\alpha_r = \frac{3(K_m + G_m) + k_r - l_r}{3(G_m + k_r)} \tag{2}$$

$$\beta_r = \frac{1}{5}\left\{\frac{4G_m + 2k_r + l_r}{3(G_m + k_r)} + \frac{4G_m}{G_m + p_r} + \frac{2\left[G_m(3K_m + G_m) + G_m(3K_m + 7G_m)\right]}{G_m(3K_m + G_m) + m_r(3K_m + 7G_m)}\right\} \tag{3}$$

$$\delta_r = \frac{1}{3}\left[n_r + 2l_r + \frac{(2k_r + l_r)(3K_m + 2G_m - l_r)}{G_m + k_r}\right] \tag{4}$$

$$\eta_r = \frac{1}{5}\left[\frac{2}{3}(n_r - l_r) + \frac{8G_m p_r}{G_m + p_r} + \frac{8m_r G_m(3K_m + 4G_m)}{3K_m(m_r + G_m) + G_m(7m_r + G_m)} + \frac{2(k_r - l_r)(2G_m + l_r)}{3(G_m + k_r)}\right] \tag{5}$$

k_r, l_r, m_r, n_r, and p_r are the Hill's elastic moduli for the reinforcing phase (CNTs). As mentioned before, the CNTs are transversely isotropic and have a stiffness matrix given below (Hill's elastic moduli)

$$\begin{pmatrix} n_r & l_r & l_r & 0 & 0 & 0 \\ l_r & k_r+m_r & k_r-m_r & 0 & 0 & 0 \\ l_r & k_r-m_r & k_r+m_r & 0 & 0 & 0 \\ 0 & 0 & 0 & p_r & 0 & 0 \\ 0 & 0 & 0 & 0 & m_r & 0 \\ 0 & 0 & 0 & 0 & 0 & p_r \end{pmatrix} \tag{6}$$

$$C_r = \begin{bmatrix} \frac{1}{E_L} & -\frac{\upsilon_{TL}}{E_T} & -\frac{\upsilon_{ZL}}{E_T} & 0 & 0 & 0 \\ -\frac{\upsilon_{LT}}{E_L} & \frac{1}{E_T} & -\frac{\upsilon_{ZT}}{E_Z} & 0 & 0 & 0 \\ -\frac{\upsilon_{LZ}}{E_L} & -\frac{\upsilon_{TZ}}{E_T} & \frac{1}{E_Z} & 0 & 0 & 0 \\ 0 & 0 & 0 & \frac{1}{G_{TZ}} & 0 & 0 \\ 0 & 0 & 0 & 0 & \frac{1}{G_{ZL}} & 0 \\ 0 & 0 & 0 & 0 & 0 & \frac{1}{G_{LT}} \end{bmatrix}^{-1} \tag{7}$$

where E_L, E_T, E_Z, G_{TZ}, G_{ZL}, G_{LT}, υ_{TZ} , υ_{ZL} and υ_{LT} are material properties of the CNT reinforced composite which can be determined from the inverse of the rule of mixture.

So, the effective Young's modulus E and Poisson's ratio υ of the composite is given by:

$$E = \frac{9KG}{3K+G} \tag{8}$$

$$\upsilon = \frac{3K-2G}{6K+2G} \tag{9}$$

3 REFINED PLATE THEORY

Consider a rectangular nanocomposite sandwich plate resting on the Winkler-Pasternak type elastic foundation with the Winkler stiffness of k_0 and shear stiffness of k_1. This sandwich plate is composed of three layers referring to rectangular coordinates (x, y, z), as shown in Fig. 2. The top and bottom layers of the plate are FG-CNTRC with thickness of h_f, and the edges of the plate are parallel to axes x and y. Also, the mid layer is made of the homogeneous polymer with thickness of h_m. The volume fractions of CNTs in n^{th} layer f_r^n (n=1, 2 3) are varied as the following:

$$f_r^1 = (1-\frac{z+h/2}{h_f})^p \times f_r^{\max} \qquad -\frac{h}{2} \langle z \langle -\frac{h_m}{2} \tag{10a}$$

$$f_r^2 = 0 \qquad -\frac{h_m}{2} \langle z \langle \frac{h_m}{2} \tag{10b}$$

$$f_r^3 = (1+\frac{z+h/2}{h_f})^p \times f_r^{\max} \qquad \frac{h_m}{2} \langle z \langle \frac{h}{2} \tag{10c}$$

where h is the total thickness of the sandwich, $p\,(0 \le p \langle \infty)$ is the volume fraction exponent and $f_r^{\max}$ is the maximum volume fraction of the CNTs in the FG-CNTRC layers and it is equal to $f_r^{\max} = 0.2$. Therefore, the effective Young's modulus E and Poisson's ratio υ of each layer are obtained from Eqs. (8-9).

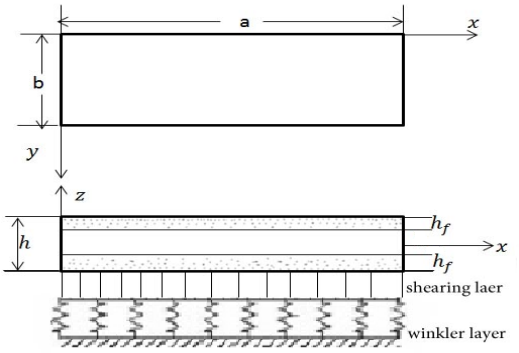

Fig.2
CNTRC sandwich plate resting on elastic foundation.

3.1 Basic assumptions

The assumptions of the present theory are as follows [25]:

a) The displacements are small in comparison with the plate thickness and thus the strains involved are infinitesimal.

b) The transverse displacement W includes two components: bending w_b and shear w_s, and these components are functions of coordinates x, y only.

$$W(x,y,z) = w_b(x,y) + w_s(x,y) \tag{11}$$

c) The transverse normal stress σ_z is negligible in comparison with the in-plane stresses σ_x and σ_y.

d) The displacements U in the x-direction and V in the y-direction consist of extension, bending, and shear components.

$$U = u + u_b + u_s, \qquad V = v + v_b + v_s \tag{12}$$

The bending components u_b and v_b are assumed to be similar to the displacements given by the classical plate theory. Therefore, the expression for u_b and v_b can be given as:

$$u_b = -z\frac{\partial w_b}{\partial x}, \qquad v_b = -z\frac{\partial w_b}{\partial y} \tag{13}$$

The shear components u_s and v_s give rise, in conjunction with w_s, to the parabolic variations of shear strains γ_{xz}, γ_{yz} and hence to shear stresses τ_{xz}, τ_{yz} across the thickness of the plate in such a way that the shear stresses τ_{xz}, τ_{yz} are zero at the top and bottom faces of the plate. Consequently, the expression for u_s and v_s can be given as:

$$u_s = \left[\frac{1}{4}z - \frac{5}{3}z\left(\frac{z}{h}\right)^2\right]\frac{\partial w_s}{\partial x}, \qquad v_s = \left[\frac{1}{4}z - \frac{5}{3}z\left(\frac{z}{h}\right)^2\right]\frac{\partial w_s}{\partial y} \tag{14}$$

3.2 Kinematics and constitutive equations

Based on the assumptions made in the preceding section, the displacement field can be obtained [25]

$$\begin{aligned} u(x,y,z) &= u_0(x,y) - z\frac{\partial w_b}{\partial x} - f(z)\frac{\partial w_s}{\partial x} \\ v(x,y,z) &= v_0(x,y) - z\frac{\partial w_b}{\partial y} - f(z)\frac{\partial w_s}{\partial y} \\ w(x,y,z) &= w_b(x,y) + w_s(x,y) \end{aligned} \tag{15}$$

where

$$f(z) = z\left[\frac{-1}{4} + \frac{5}{3}\left(\frac{z}{h}\right)^2\right] \tag{16}$$

The strains associated with the displacements in Eq. (15) are:

$$\begin{aligned} &\varepsilon_x = \varepsilon_x^0 + zk_x^b + f(z)k_x^s \ , \ \varepsilon_y = \varepsilon_y^0 + zk_y^b + f(z)k_y^s \\ &\gamma_{xy} = \gamma_{xy}^0 + zk_{xy}^b + f(z)k_{xy}^s \ , \ \gamma_{yz} = g(z)\gamma_{yz}^s \ , \ \gamma_{xz} = g(z)\gamma_{xz}^s \\ &\varepsilon_z = 0 \end{aligned} \tag{17}$$

where

$$\begin{aligned} &\varepsilon_x^0 = \frac{\partial u_0}{\partial x}, \qquad k_x^b = -\frac{\partial^2 w_b}{\partial x^2}, \qquad k_x^s = -\frac{\partial^2 w_s}{\partial x^2} \\ &\varepsilon_y^0 = \frac{\partial v_0}{\partial y}, \qquad k_y^b = -\frac{\partial^2 w_b}{\partial y^2}, \qquad k_y^s = -\frac{\partial^2 w_s}{\partial y^2} \\ &\gamma_{xy}^0 = \frac{\partial u_0}{\partial y} + \frac{\partial v_0}{\partial x}, \quad k_{xy}^0 = -2\frac{\partial^2 w_b}{\partial x \partial y}, \quad k_{xy}^s = -2\frac{\partial^2 w_s}{\partial x \partial y} \\ &\gamma_{yz}^0 = \frac{\partial w_s}{\partial y}, \qquad \gamma_{xz}^s = \frac{\partial w_s}{\partial x}, \qquad g(z) = 1 - \frac{df(z)}{dz} \end{aligned} \tag{18}$$

For elastic and isotropic materials, the constitutive relations can be written as:

$$\begin{Bmatrix} \sigma_x \\ \sigma_y \\ \tau_{xy} \end{Bmatrix}^{(n)} = \begin{bmatrix} Q_{11} & Q_{12} & 0 \\ Q_{12} & Q_{22} & 0 \\ 0 & 0 & Q_{66} \end{bmatrix}^{(n)} \begin{Bmatrix} \varepsilon_x \\ \varepsilon_y \\ \gamma_{xy} \end{Bmatrix}^{(n)} \qquad \begin{Bmatrix} \tau_{yz} \\ \tau_{zx} \end{Bmatrix}^{(n)} = \begin{bmatrix} Q_{44} & 0 \\ 0 & Q_{55} \end{bmatrix}^{(n)} \begin{Bmatrix} \gamma_{yz} \\ \gamma_{zx} \end{Bmatrix}^{(n)} \tag{19}$$

where n is the number of each layers, $(\sigma_x, \sigma_y, \tau_{xy}, \tau_{yz}, \tau_{xz})$ and $(\varepsilon_x, \varepsilon_y, \gamma_{xy}, \gamma_{yz}, \gamma_{zx})$ are the stress and strain components, respectively. Using the material properties defined in Eq. (10), stiffness coefficients, Q_{ij}, can be expressed as:

$$Q_{11} = Q_{22} = \frac{E}{1-\nu^2}, \qquad Q_{12} = \frac{\nu E}{1-\nu^2} \qquad Q_{66} = Q_{44} = Q_{55} = \frac{E}{2(1+\nu)} \tag{20}$$

3.3 Governing equations

Using Hamilton's energy principle derives the motion equation of the isotropic plate:

$$\delta\int_{t_1}^{t_2}(U+U_F-K)dt=0 \tag{21}$$

where U is the strain energy, K is the kinetic energy of the isotropic plate, U_F is the strain energy of foundation. Employing the minimum of the total energy principle leads to a general equation of motion and boundary conditions. Taking the variation of the above equation and integrating by parts:

$$\int_{t_1}^{t_2}\Big[\int_v\Big[\sigma_x\delta\varepsilon_x+\sigma_y\delta\varepsilon_y+\tau_{xy}\delta\gamma_{xy}+\tau_{yz}\delta\gamma_{yz}+\tau_{zx}\delta\gamma_{zx}-\rho(\ddot{u}\delta u+\ddot{v}\delta v+\ddot{w}\delta w)\Big]dv+\int_A f_e\delta w dA\ \Big]dt=0 \tag{22}$$

where represents the second derivative with respect to time and f_e is the density of reaction force of foundation. For the Pasternak foundation model:

$$f_e=k_0w-k_1\nabla^2w \tag{23}$$

The equations of motion can be obtained by substitution of Eqs. (15) and (17) into Eq. (22) and by considering following assumptions. The stress resultants *N,M,S* and the mass moments of inertia are defined by:

$$\begin{bmatrix}N_x & N_y & N_{xy}\\ M_x^b & M_y^b & M_{xy}^b\\ M_x^S & M_y^S & M_{xy}^s\end{bmatrix}=\sum_{n=1}^{3}\int_{h_n}^{h_{n+1}}(\sigma_x,\sigma_y,\tau_{xy})^{(n)}\begin{pmatrix}1\\ z\\ f(z)\end{pmatrix}dz \tag{24a}$$

$$(S_{xz}^s,S_{yz}^s)=\sum_{n=1}^{3}\int_{h_n}^{h_{n+1}}(\tau_{xz},\tau_{yz})^{(n)}g(z)dz \tag{24b}$$

$$(I_1,I_2,I_3,I_4,I_5,I_6)=\sum_{n=1}^{3}\int_{h_n}^{h_{n+1}}\rho(z)(1,z,z^2,f(z),zf(z),(f(z))^2dz \tag{24c}$$

where h_{n+1} and h_n are the top and bottom *z*-coordinates of the *nth* layer. So, the equation of motion can be written as:

$$\delta u_0:\quad N_{x,x}+N_{xy,y}=I_2\ddot{w}_{b,x}+I_4\ddot{w}_{s,x}-I_1\ddot{u}_0 \tag{25a}$$

$$\delta v_0:\quad N_{y,y}+N_{xy,x}=I_2\ddot{w}_{b,y}+I_4\ddot{w}y-I_1\ddot{v}_0 \tag{25b}$$

$$\begin{aligned}\delta w_b:\quad & M_{x,xx}^b+M_{y,yy}^b+2M_{xy,xy}^b-(k_0w-k_1\nabla^2w)\\ & =I_3(\ddot{w}_{b,xx}+\ddot{w}_{b,yy})+I_5(\ddot{w}_{s,xx}+\ddot{w}_{s,yy})-I_2(\ddot{u}_{0,x}+\ddot{v}_{0,y})-I_1(\ddot{w}_b+\ddot{w}_s)\end{aligned} \tag{25c}$$

$$\begin{aligned}\delta w_s:\quad & M_{x,xx}^s+M_{y,yy}^s+2M_{xy,xy}^s+S_{yz,y}^s+S_{xz,x}^s-(k_0w-k_1\nabla^2w)\\ & =I_5(\ddot{w}_{b,xx}+\ddot{w}_{b,yy})+I_6(\ddot{w}_{s,xx}+\ddot{w}_{s,yy})-I_4(\ddot{u}_{0,x}+\ddot{v}_{0,y})-I_1(\ddot{w}_b+\ddot{w}_s)\end{aligned} \tag{25d}$$

Substituting Eq. (19) into Eq. (24) and integrating through the thickness of the plate, the stress resultants are given as:

$$\begin{Bmatrix} N \\ M^b \\ M^s \end{Bmatrix} = \begin{bmatrix} A & B & B^s \\ B & D & D^s \\ B^s & D^s & H^s \end{bmatrix} \begin{Bmatrix} \varepsilon \\ k^b \\ k^s \end{Bmatrix}, \qquad S = A^s \gamma \tag{26}$$

where

$$N = \left\{N_x, N_y, N_{xy}\right\}^T, \qquad M^b = \left\{M_x^b, M_y^b, M_{xy}^b\right\}^T, \qquad M^s = \left\{M_x^s, M_y^s, M_{xy}^s\right\}^T \tag{27}$$

$$\varepsilon = \left\{\varepsilon_x^0, \varepsilon_y^0, \varepsilon_{xy}^0\right\}^T, \qquad k^b = \left\{k_x^b, k_y^b, k_{xy}^b\right\}^T, \qquad k^s = \left\{k_x^s, k_y^s, k_{xy}^s\right\}^T \tag{28}$$

$$S = \left\{S_{xz}^s, S_{yz}^s\right\}^1, \qquad \gamma = \left\{\gamma_{xy}, \gamma_{yz}\right\}^1 \tag{29}$$

$$\begin{aligned} A &= \begin{bmatrix} A_{11} & A_{12} & 0 \\ A_{12} & A_{22} & 0 \\ 0 & 0 & A_{66} \end{bmatrix} \qquad B = \begin{bmatrix} B_{11} & B_{12} & 0 \\ B_{12} & B_{22} & 0 \\ 0 & 0 & B_{66} \end{bmatrix} \qquad D = \begin{bmatrix} D_{11} & D_{12} & 0 \\ D_{12} & D_{22} & 0 \\ 0 & 0 & D_{66} \end{bmatrix} \\ B^s &= \begin{bmatrix} B_{11}^s & B_{12}^s & 0 \\ B_{12}^s & B_{22}^s & 0 \\ 0 & 0 & B_{66}^s \end{bmatrix} \qquad D^s = \begin{bmatrix} D_{11}^s & D_{12}^s & 0 \\ D_{12}^s & D_{22}^s & 0 \\ 0 & 0 & D_{66}^s \end{bmatrix} \qquad H^s = \begin{bmatrix} H_{11}^s & H_{12}^s & 0 \\ H_{12}^s & H_{22}^s & 0 \\ 0 & 0 & H_{66}^s \end{bmatrix} \\ A^s &= \begin{bmatrix} A_{44}^s & 0 \\ 0 & A_{55}^s \end{bmatrix} \end{aligned} \tag{30}$$

And stiffness components are given as:

$$\begin{aligned} &\left\{A_{ij}, B_{ij}, D_{ij}, B_{ij}^s, D_{ij}^s, H_{ij}^s\right\} = \sum_{n=1}^{3} \int_{h_n}^{h_{n+1}} \left\{1, z, z^2, f(z), zf(z), (f(z))^2\right\} Q_{ij} dz \qquad (i, j = 1, 2, 6) \\ &A_{44}^s = A_{55}^s = \sum_{n=1}^{3} \int_{h_n}^{h_{n+1}} \frac{E(z)}{2(1+\nu)} \left[g(z)\right]^2 dz \end{aligned} \tag{31}$$

3.4 Navier's solution for simply supported rectangular sandwich plates

Rectangular sandwich plates are generally classified in accordance with the type support used. We are here concerned with the analytical solutions of Eq. (25) for simply supported FG-CNTRC sandwich plate. The following boundary conditions are imposed at the side edges [25]:

$$\begin{aligned} &v_0(0,y) = w_b(0,y) = w_s(0,y) = \frac{\partial w_b}{\partial y}(0,y) = \frac{\partial w_s}{\partial y}(0,y) = 0 \\ &v_0(a,y) = w_b(a,y) = w_s(a,y) = \frac{\partial w_b}{\partial y}(a,y) = \frac{\partial w_s}{\partial y}(a,y) = 0 \\ &u_0(x,0) = w_b(x,0) = w_s(x,0) = \frac{\partial w_b}{\partial x}(x,0) = \frac{\partial w_s}{\partial x}(x,0) = 0 \\ &u_0(x,b) = w_b(x,b) = w_s(x,b) = \frac{\partial w_b}{\partial x}(x,b) = \frac{\partial w_s}{\partial x}(x,b) = 0 \\ &N_x(0,y) = M_x^b(0,y) = M_x^s(0,y) = N_x(a,y) = M_x^b(a,y) = M_x^s(a,y) = 0 \\ &N_x(x,0) = M_x^b(x,0) = M_x^s(x,0) = N_x(x,b) = M_x^b(x,b) = M_x^s(x,b) = 0 \end{aligned} \tag{32}$$

The displacement functions that satisfy the equations of boundary conditions (Eq.(32)) are selected as the following Fourier series:

$$\begin{Bmatrix} u_0 \\ v_0 \\ w_b \\ w_s \end{Bmatrix} = \sum_{m=1}^{\infty}\sum_{n=1}^{\infty} \begin{Bmatrix} u_{mn}\cos(\lambda x)\sin(\mu y)e^{iwt} \\ v_{mn}\sin(\lambda x)\cos(\mu y)e^{iwt} \\ w_{bmn}\sin(\lambda x)\sin(\mu y)e^{iwt} \\ w_{smn}\sin(\lambda x)\sin(\mu y)e^{iwt} \end{Bmatrix} \tag{33}$$

where u_{mn}, v_{mn}, w_{bmn} and w_{smn} are the arbitrary parameters to be determined, ω is the eigen frequency associated with (*m*,*n*) *th* eigen mode, $\lambda = \frac{m\pi}{a}$ and $\mu = \frac{n\pi}{b}$. Substituting Eq. (33) into equations of motion (25) we get the below eigenvalue equations for any fixed value of *m* and *n*:

$$([k]-\omega^2[M])\{\Delta\} = 0 \tag{34}$$

where

$$\{\Delta\}\begin{Bmatrix} u_{mn} \\ v_{mn} \\ w_{bmn} \\ w_{smn} \end{Bmatrix} \qquad k = \begin{bmatrix} a_{11} & a_{12} & a_{13} & a_{14} \\ a_{12} & a_{22} & a_{23} & a_{24} \\ a_{13} & a_{23} & a_{33} & a_{34} \\ a_{14} & a_{24} & a_{34} & a_{24} \end{bmatrix} \qquad M = \begin{bmatrix} m_{11} & 0 & m_{13} & m_{14} \\ 0 & m_{22} & m_{23} & m_{24} \\ m_{13} & m_{23} & m_{33} & m_{34} \\ m_{14} & m_{24} & m_{34} & m_{44} \end{bmatrix} \tag{35}$$

And the elements of the coefficient matrix *k* and *M* are given in Appendix A. To avoid of trivial solution of Eq. (34), the following equations should be solved:

$$\left|[k]-\omega^2[M]\right| = 0 \tag{36}$$

Or, with pre-multiplying Eq. (36) by $[M]^{-1}$, becomes

$$\left|[M]^{-1}[k]-\omega^2[I]\right| = 0 \tag{37}$$

The natural frequencies (ω) can be derived by solving of this equation.

4 RESULTS AND DISCUSSIONS

In this section, at first the accuracy of applied method is examined by comparing obtained results of FGM plates with reported results in the literatures and then effects of sandwich plates dimension, elastic foundation parameters, CNTs volume fraction and their variation patterns are investigated on the frequency parameters of FG-CNTRC sandwich plates.

4.1 Validation of models

At first, to validate the vibration analyses, first normalized frequency parameters (Ω_{11}) of isotropic FGM plates are presented for various values of volume fraction exponent, *p*, and ratio of length to thickness, *a/h*, in Table 1. The normalized natural frequency is defined as:

$$\Omega_{mn} = \omega_{mn} a^2 \sqrt{\frac{\rho_m h}{D_m}} \tag{38}$$

where

$$D_m = \frac{E_m h^3}{12(1-\nu^2)} \tag{39}$$

The subscript of m is used for metal in the applied FGM plate. In these plates, values of the elastic foundation are given as zero. The comparisons show that the present results agree very well with other available solutions. Further validation of the present results is shown for FGM plates resting on elastic foundation in Table 2. The normalized elastic foundation parameters are defined as $K_0 = \frac{k_0 a^4}{D_m}$ and $K_1 = \frac{k_1 a^2}{D_m}$. In this table, a comparison is made for different values of the elastic foundation parameters and ratio of h/a. As observed, there is a good agreement between the results too.

Table 1
Comparison of the first frequency parameters of square isotropic FGM plates for various values of p and a/h.

a/h	Theory	p=0	p=1	p=4	p=10
2	Matsunaga (2008)	0.9400	0.7477	0.5997	0.5460
	Ait Atmane et al. (2010)	0.9300	0.7725	0.6244	0.5573
	Present	0.9304	0.7360	0.5928	0.5417
5	Matsunaga (2008)	0.2121	0.1640	0.1383	0.1306
	Ait Atmane et al. (2010)	0.2113	0.1740	0.1520	0.1369
	Present	0.2113	0.1631	0.1378	0.1301
10	Matsunaga (2008)	0.05777	0.04427	0.03811	0.03642
	Ait Atmane et al. (2010)	0.05770	0.04718	0.04210	0.03832
	Present	0.05769	0.04419	0.03807	0.03637

Table 2
Comparison of the first frequency parameters of square isotropic FGM plates resting on elastic foundation for various values of K_0, K_1 and h/a.

h/a	K_0 , K_1	Akhavan et al. (2009)	Ait Atmane et al. (2010)	Present
0.001	0.0	19.7391	19.7392	19.7396
	100.10	26.2112	26.2112	26.2115
	1000.100	57.9961	57.9962	57.9963
0.1	0.0	19.0840	19.0658	19.0658
	100.10	25.6368	25.6236	25.6235
	1000.100	57.3969	57.3923	57.3922
0.2	0.0	17.5055	17.4531	17.4530
	100.10	24.3074	24.2728	24.2728
	1000.100	56.0359	56.0311	56.0363

Table 3
Three normalized frequency parameters of FG-CNTRC sandwich square plates for various values of a/h and p (h/h_f=3 and n=1).

a/h	m	p						
		0	0.01	0.1	1	5	10	20
2	1	89.2953	88.6761	83.5435	53.9178	24.4815	19.6993	18.1649
	2	157.6137	156.4234	146.6261	92.3052	41.0945	32.8613	30.5083
	3	238.7703	236.9411	221.9257	139.6636	62.0514	49.0900	45.4684
5	1	144.3772	143.6796	137.8069	99.9862	51.5519	41.2564	35.8894
	2	296.8109	295.0554	280.3743	190.5451	90.7716	73.0240	65.9360
	3	482.0430	478.8072	451.9273	294.7039	134.9870	108.6693	99.8395
10	1	166.8645	166.2409	160.9811	126.3465	74.5209	58.8787	47.8630
	2	385.6784	383.9938	369.7884	276.9041	149.7368	119.3423	101.4107
	3	694.1500	690.6235	660.9720	471.9599	238.1464	190.9032	167.8024

4.2 Vibration of the FG-CNTRC sandwich plates

After validation of the applied method, vibration behaviors of FG-CNTRC sandwich plates are investigated. The top and bottom layer are considered FG-CNTRC plates and made of Poly (methyl- methacrylate, referred as PMMA) as matrix, with CNT as fibers. PMMA is an isotropic material with $E^m = 2.5\,GPa$, $\upsilon^m = 0.34$ and $\rho^m = 1150\,Kg/m^3$. The (10,10) single-walled CNTs are selected as reinforcements. The adopted material properties for SWCNT are: $E_1^{CNT} = 5.6466\,TPa$, $E_2^{CNT} = 7.0800\,TPa$, $G_{12}^{CNT} = 1.9445\,TPa$, $\upsilon^{CNT} = 0.175$ and $\rho^{CNT} = 1400\,Kg/m^3$ [14]. Table 3. reports three normalized frequency parameters (for n=1 and m=1, 2, 3) of FG-CNTRC sandwich square plates (a/b=1) with h/h_f=3 and for various values of a/h and volume fraction exponent, p. As observed, increasing of the ratio of a/h increases all the frequency parameters of the sandwich square plates, also increasing of the volume fraction exponent decreases the frequencies because of the CNT volume was decreased.

In Table 4. the effects of h/a ratio and elastic foundation parameters (based on the mechanical properties of PMMA) are investigated for FG-CNTRC sandwich square plates with h/h_f=3 and exponent of p=0.01. It can be seen that, increasing of the h/a ratio leads to decrease in the frequency parameter; also elastic foundation increases the frequencies and improving of their parameters increase the frequencies.

Table 4
Frequency parameters of FG-CNTRC sandwich square plates resting on elastic foundation for various values of K_0, $K_1$and h/a (h/h_f=3 and p=0.01.)

h/a	K_0	K_1	Ω
0.001	0	0	176.9648
	100	10	177.7798
	1000	100	184.9529
0.1	0	0	166.2409
	100	10	167.0968
	1000	100	174.6111
0.2	0	0	143.6796
	100	10	144.6517
	1000	100	153.1230

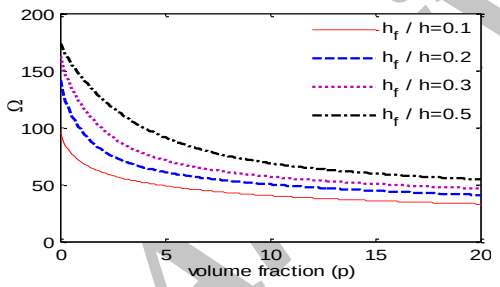

Fig.3
First frequency parameters versus volume fraction values of CNTRC sandwich plates for various values of h_f (a/b=1, a/h=10 and $k_0 = k_1 = 0$).

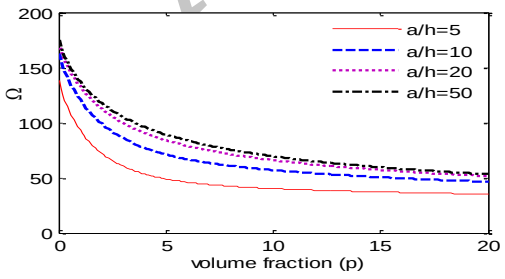

Fig.4
First frequency parameters versus volume fraction values of CNTRC sandwich plates for various values of a/h (a/b=1, h_f/h=0.3 and $k_0 = k_1 = 0$).

The effects of FG-CNTRC layers thickness, h_f, sandwich length, a, and volume fraction exponent on the first frequency parameter are investigated in Figs. 3-4. No elastic foundation is considered for these sandwich plates and the ratios of a/b and a/h are equal to 1 and 10, respectively. As observed in Fig. 3, increasing of the volume fraction exponent or decreasing of the FG-CNTRC layers thickness decrease first frequency parameter because of the

decreasing in the CNTs volume fraction of sandwich plates. Also, Fig. 4 shows increasing of the a/h increases the first frequency parameter for these sandwich plates with h_f/h =0.3.

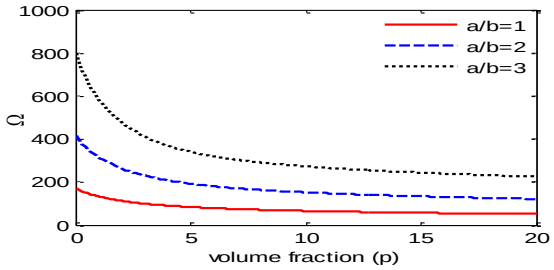

Fig.5
First frequency parameters versus volume fraction values of CNTRC sandwich plates for various values of a/b (a/h=20, h_f/h=0.3 and $k_0 = k_1 = 0$).

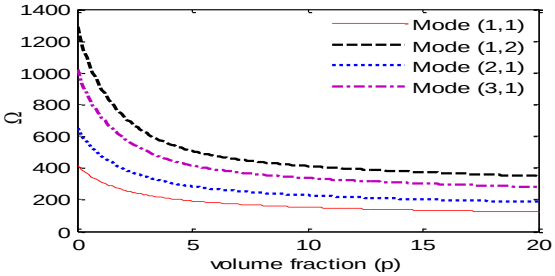

Fig.6
Various modes of frequency parameters versus volume fraction values of CNTRC sandwich plates (a/b=2, h_f/h=0.3, a/h=20 and $k_0 = k_1 = 0$).

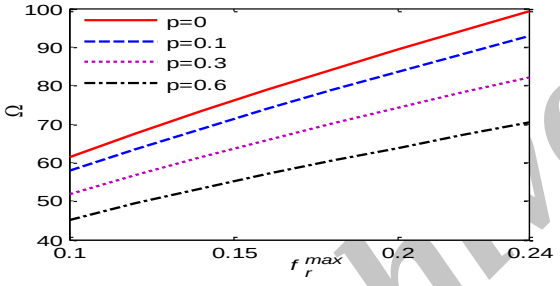

Fig.7
First frequency parameters versus maximum values of CNT volume fraction for CNTRC sandwich plates with various values of p (a/b=1, a/h=2, h/h_f=3 and $k_0 = k_1 = 0$).

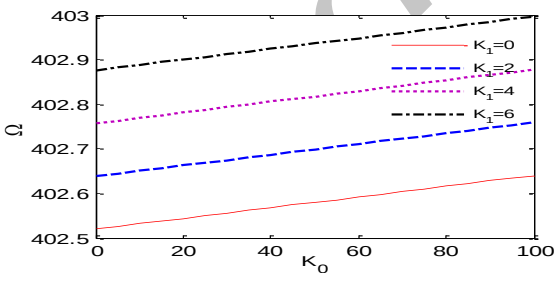

Fig.8
First frequency parameters versus shear parameter values of elastic foundation for CNTRC sandwich plates with various values of k_1 (a/b=2, a/h=20, h_f/h=0.3 and $p = 0.1$).

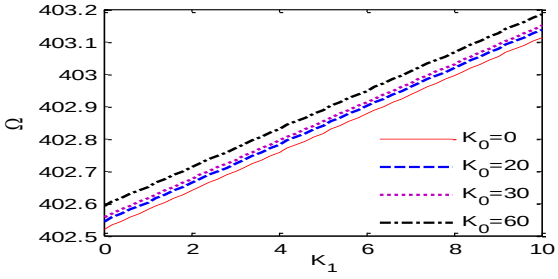

Fig.9
First frequency parameters versus Winkler parameter values of elastic foundation for CNTRC sandwich plates with various values of k_0 (a/b=2, a/h=20, h_f/h=0.3 and $p = 0.1$).

First frequency parameters are shown in Fig. 5 for these sandwich plates with a/h=20, h_f/h =0.3 and various values of volume fraction exponent and a/b. This figure shows that increasing of a/b ratio increases frequency parameter. Consider other FG-CNTRC sandwich plates with a/b=2, a/h=20, h_f/h =0.3 and without elastic foundation. Fig. 6 shows variations of $\Omega_{11},\Omega_{12},\Omega_{21},\Omega_{31}$ versus volume fraction exponent in these sandwich plates. This figure shows that frequency parameters are decreased by increasing p. In the other case, consider square nanocomposite sandwich plates with a/h=2, h/h_f =3 and with various values of p and $f_r^{\max}$ same as previous ones. Fig. 7 shows that increasing of maximum value of CNT volume fraction increases the natural frequency. Finally, effects of elastic foundation parameters of the sandwich plates with a/b=2, a/h=20, h_f/h =0.3 and p=0.1, are investigated on the first frequency parameters in Figs. 8-9. These figures reveal that increasing the foundation parameters increase the first frequency parameter and the shear parameter (k_0) has more influence than the other one (k_1).

5 CONCLUSIONS

In this paper by using a refined plate theory, the effects of various parameters were investigated on the natural frequency of the FG-CNTRC sandwich plates. The sandwich plates were simply supported and the Winkler/ Pasternak elastic foundation were considered for them. The nanotubes were considered straight with randomly oriented and Mori–Tanaka approach was used to estimate the mechanical properties of nanocomposites. The motion equation was derived by Hamilton's energy principle and Navier's method solved by this equation. The following results were obtained from this analysis:

- Increasing of the ratios of a/h or a/b, increase the frequency parameters of the sandwich plates.
- Increasing of the volume fraction exponent, (p) or decreasing of the FG-CNTRC layers thickness (h_f) decrease frequency parameter because of the decreasing in the CNT volume of sandwich plates.
- Increasing of maximum value of CNT volume fraction increases frequency parameter.
- Increasing in the foundation parameters increase the first frequency parameter and the shear parameter (k_0) has more influence than the other one (k_1).

APPENDIX

$$
\begin{aligned}
a_{11} &= (A_{11}\lambda^2 + A_{66}\mu^2)\\
a_{12} &= (A_{12} + A_{66})\mu\lambda\\
a_{13} &= -(B_{11}\lambda^2 + \mu^2(B_{12} + 2B_{66}))\lambda\\
a_{14} &= -(B^s_{11}\lambda^2 + \mu^2(B^s_{12} + 2B^s_{66}))\lambda\\
a_{22} &= (A_{22}\mu^2 + A_{66}\lambda^2)\\
a_{23} &= -(\lambda^2(B_{12} + 2B_{66}) + B_{22}\mu^2)\mu\\
a_{24} &= -(\lambda^2(B^S_{12} + 2B^s_{66}) + B^s_{22}\mu^2)\mu\\
a_{33} &= (D_{11}\lambda^4 + 2D_{12}\lambda^2\mu^2 + D_{22}\mu^4 + 4D_{66}\lambda^2\mu^2 + k_0 + k_1(\lambda^2 + \mu^2)\\
a_{34} &= (D^s_{11}\lambda^4 + 2D^s_{12}\lambda^2\mu^2 + D^s_{22}\mu^4 + 4D^s_{66}\lambda^2\mu^2 + k_0 + k_1(\lambda^2 + \mu^2)\\
a_{44} &= (H^s_{11}\lambda^4 + 2H^s_{12}\lambda^2\mu^2 + H^s_{22}\mu^4 + 4H^s_{66}\lambda^2\mu^2 + k_0 + k_1(\lambda^2 + \mu^2) + \mu^2 A^s_{44} + \lambda^2 A^s_{55}\\
m_{11} &= m_{22} = m_{44} = -I_1\\
m_{13} &= I_2\lambda m_{14} = I_4\lambda m_{23} = I_2\lambda m_{24} = I_4\mu\\
m_{33} &= -(I_3(\lambda^2 + \mu^2) + I_1) m_{34} = -(I_5(\lambda^2 + \mu^2) + I_1)
\end{aligned}
$$

REFERENCES

[1] Wagner H.D., Lourie O., Feldman Y., 1997, Stress-induced fragmentation of multiwall carbon nanotubes in a polymer matrix, *Applied Physics Letters* **72**: 188-190.

[2] Griebel M., Hamaekers J., 2004, Molecular dynamic simulations of the elastic moduli of polymer-carbon nanotube composites, *Computer Methods in Applied Mechanics and Engineering* **193**: 1773-1788.

[3] Fidelus J.D., Wiesel E., Gojny F.H., Schulte K., Wagner H.D., 2005, Thermo-mechanical properties of randomly oriented carbon/epoxy nanocomposites, *Composite Part A* **36**: 1555-1561.

[4] Song Y.S., Youn J.R., 2006, Modeling of effective elastic properties for polymer based carbon nanotube composites, *Polymer* **47**:1741-1748.

[5] Han Y., Elliott J., 2007, Molecular dynamics simulations of the elastic properties of polymer/carbon nanotube composites, *Computational Materials Science* **39**: 315-323.

[6] Zhu R., Pan E., Roy A.K., 2007, Molecular dynamics study of the stress–strain behavior of carbon-nanotube reinforced Epon 862 composites, *Materials Science and Engineering A* **447**: 51-57.

[7] Manchado M.A.L., Valentini L., Biagiotti J., Kenny J.M., 2005, Thermal and mechanical properties of single-walled carbon nanotubes-polypropylene composites prepared by melt processing, *Carbon* **43**: 1499-1505.

[8] Qian D., Dickey E.C., Andrews R., Rantell T., 2000, Load transfer and deformation mechanisms in carbon nanotube–polystyrene composites, *Applied Physics Letters* **76**: 2868-2870.

[9] Mokashi V.V., Qian D., Liu Y.J., 2007, A study on the tensile response and fracture in carbon nanotube-based composites using molecular mechanics, *Composites Science and Technology* **67**: 530-540.

[10] Wuite J., Adali S., 2005, Deflection and stress behaviour of nanocomposite reinforced beams using a multiscale analysis, *Composite Structures* **71**: 388-396.

[11] Reddy J.N., 2000, Analysis of functionally graded plates, I*nternational Journal for Numerical Methods in Engineering* **47**: 663-684.

[12] Cheng Z.Q., Batra R.C., 2000, Deflection relationships between the homogeneous Kirchhoff plate theory and different functionally graded plate theories, *Archive of Mechanics* **52**:143-158.

[13] Cheng Z.Q., Batra R.C., 2000, Exact correspondence between eigenvalues of membranes and functionallygraded simplysupported polygonal plates, *Journal of Sound and Vibration* **229**: 879-895.

[14] Shen H.S., 2011, Postbuckling of nanotube-reinforced composite cylindrical shells in thermal environments, Part I: Axially-loaded shells, *Composite Structures* **93**: 2096-2108.

[15] Ke L.L., Yang J., Kitipornchai S., 2010, Nonlinear free vibration of functionally graded carbon nanotube-reinforced composite beams, *Composite Structures* **92**: 676-683.

[16] Mori T., Tanaka K., 1973, Average stress in matrix and average elastic energy of materials with Misfitting inclusions, *Acta Metallurgica* **21**: 571-574.

[17] Yas M.H., Heshmati M., 2012, Dynamic analysis of functionally graded nanocomposite beams reinforced by randomly oriented carbon nanotube under the action of moving load, *Applied Mathematical Modelling* **36**: 1371-1394.

[18] Sobhani Aragh B., Nasrollah Barati A.H., Hedayati H., 2012, Eshelby–Mori–Tanaka approach for vibrational behavior of continuously graded carbon nanotube–reinforced cylindrical panels, *Composites Part B* **43**: 1943-1954.

[19] Pourasghar A., Yas M.H., Kamarian S., 2013, Local aggregation effect of CNT on the vibrational behavior of four-parameter continuous grading nanotube-reinforced cylindrical panels, *Polymer Composites* **34**: 707-721.

[20] Moradi-Dastjerdi R., Pourasghar A., Foroutan M., 2013, The effects of carbon nanotube orientation and aggregation on vibrational behavior of functionally graded nanocomposite cylinders by a mesh-free method, *Acta Mechanica* **224**: 2817-2832.

[21] Pasternak P.L., 1954, *On a New Method of Analysis of an Elastic Foundation by Means of Two Foundation Constants*, Cosudarstrennoe Izdatelstvo Literaturi po Stroitelstvu i Arkhitekture, Moscow, USSR.

[22] Pourasghar A., Kamarian S., 2013, Three-dimensional solution for the vibration analysis of functionally graded multiwalled carbon nanotubes/phenolic nanocomposite cylindrical panels on elastic foundation, *Polymer Composites* **34**: 2040-2048.

[23] Zenkour AM., 2006, Generalized shear deformation theory for bending analysis of functionally graded plates, *Applied Mathematical Modelling* **30**: 67-84.

[24] Zenkour AM., 2009, The refined sinusoidal theory for FGM plates on elastic foundations, *International Journal of Mechanical Sciences* **51**: 869-880.

[25] Merdaci S., Tounsi A., A.Houari M.S., Mechab I., Hebali H., Benyoucef S., 2011, Two new refined shear displacement models for functionally graded sandwich plates, *Archive of Applied Mechanics* **81**:1507-1522.

[26] Thai H.T., Choi D.H., 2011, A refined plate theory for functionally graded plates resting on elastic foundation, *Composites Science and Technology* **71**: 1850-1858.

[27] Akavci SS., 2007, Buckling and free vibration analysis of symmetric and antisymmetric laminated composite plates on an elastic foundation, *Journal of Reinforced Plastics and Composites* **26**: 1907-1919.

[28] Benyoucef S., Mechab I., Tounsi A., Fekrar A., Ait Atmane H., Adda Bedia EA., 2010, Bending of thick functionally graded plates resting on Winkler-Pasternak elastic foundations, *Mechanics of Composite Materials* **46**: 425-434.

[29] Ait Atmane H., Tounsi A., Mechab I., Adda Bedia EA., 2010, Free vibration analysis of functionally graded plates resting on Winkler-Pasternak elastic foundations using a new shear deformation theory, *International Journal of Mechanics and Materials in Design* **6**: 113-121.

[30] Shi D.L., Feng X.Q., Yonggang Y.H., Hwang K.C., Gao H., 2004, The effect of nanotube waviness and agglomeration on the elasticproperty of carbon nanotube reinforced composites, *Journal of Engineering Materials and Technology* **126**: 250-257.

[31] Matsunaga H., 2008, Free vibration and stability of functionally graded plates according to a 2D higher-order deformation theory, *Composite Structures* **82**: 499-512.

[32] Akhavan H., Hosseini-Hashemi Sh., Rokni Damavandi Taher H., Alibeigloo A., Vahabi Sh., 2009, Exact solutions for rectangular Mindlin plates under in-plane loads resting on Pasternak elastic foundation. Part II: Frequency analysis, *Computational Materials Science* **44**: 951-961.